Plasmonic Nanoparticles

Deutsche Ausgabe: DOI: 10.1002/ange.201608271
Internationale Ausgabe: DOI: 10.1002/anie.201608271

Dry Sintering Meets Wet Silver-Ion "Soldering": Charge-Transfer Plasmon Engineering of Solution-Assembled Gold Nanodimers From Visible to Near-Infrared I and II Regions

*Lingling Fang, Yueliang Wang, Miao Liu, Ming Gong, An Xu, and Zhaoxiang Deng**

Abstract: *Achieving highly tunable and localized surface plasmon resonance up to near infrared (NIR) regions is a key target in nanoplasmonics. In particular, a self-assembly process capable of producing highly uniform and solution-processable nanomaterials with tailor-made plasmonic properties is lacking. We herein address this problem through a conjunctive use of wet Ag^+ soldering and dry thermal sintering to produce nanodimer-derived structures with precisely engineered charge-transfer plasmon (CTP). The sintered dimers are water soluble, featuring gradually shifted CTP spanning an 800 nm wavelength range (up to NIR II). Upon silica removal, the products are grafted by DNA to offer surface functionality. This process is also adaptable to DNA-linked AuNP dimers toward plasmonic meta-materials via DNA-guided soldering and sintering.*

Localized surface plasmon resonance (LSPR) is a coherent, collective spatial oscillation of free electrons in a nanostructured material (typically Au, Ag, or Cu metal).[1] A plasmonic structure therefore selectively absorbs and scatters light at specific resonance wavelengths. In the case of a self-assembled structure, LSPR is not only related to the shape, size, charge, and dielectric environment[2] of its structural units but also strongly dependent on its spatial order and interparticle gap[3] or conductive junction (CJ).[4] Plasmonic coupling of nanoparticles is important to achieve tunable optical properties, which can be understood by a plasmon hybridization model.[3b,5] This enables LSPR to be controlled by accurately positioning plasmonic units at pre-determined sites, and in this regard DNA nanotechnology offers an especially powerful positioning tool.[6] Pursuits along this direction would create chances toward surface enhanced spectroscopy,[6d,e,7] molecular sensing,[8] bio-imaging/therapy,[9] light harvesting,[10] hot-electron catalysis,[11] and nonlinear optical devices.[12]

Nanoparticle clusters are super-assemblies of solution-synthesized colloidal particles, among which Au nanoparticle (AuNP) dimers are the most basic and simplest form. Theoretical modelling has revealed a widely tunable longitudinal LSPR of Au dimers[3b,13] sensitive to the gap size (untouched dimer) or junction width (coalesced dimer). With a reduced interparticle gap, the longitudinal LSPR redshifts before a quantum tunneling[3b] is reached and then blueshifts after a charge-transfer plasmon (CTP) appears for coalesced particles. The CTP represents light frequency oscillations of free electrons across a conductive interparticle junction. As a result, electrical neutrality is only valid for the involved particles as a whole (not for each particle). This unique plasmon can lead to advanced devices including terahertz photonic devices[14] and ultrafast nanoswitches.[15] While the interparticle gap is controllable by molecular linkers, such as DNA, to realize plasmonic tuning,[16] it is very hard, due to a charge-transport dilemma of solution-processed materials,[17] to make conductive interparticle junctions by a bulk chemical process. To obtain such physically interfaced structures, Nam et al. synthesized Au–Ag nano-snowmen using DNA-grafted AuNPs for silver deposition.[18] Lu et al. made use of DNA adsorption to control the overgrowth of Au nanorods into dumbbell structures.[19] Sun et al. built gold–silver bi-domain dimers based on a heterogeneous silver nucleation on gold.[20] Others often relied on lithography techniques[21] or e-beam induced "melting"[22] under transmission electron microscope (TEM) to realize coalesced structures.

We herein report a highly reliable process (Figure 1) to realize a widely tuned CTP of AuNP dimers from visible to

[*] L. L. Fang, Y. L. Wang, M. Liu, Prof. Z. X. Deng
CAS Key Laboratory of Soft Matter Chemistry
University of Science and Technology of China
Hefei, Anhui 230026 (China)
E-mail: zhxdeng@ustc.edu.cn
Prof. M. Gong
Engineering and Materials Science Experiment Center, University of Science and Technology of China
Hefei, Anhui 230027 (China)
Prof. A. Xu
Key Laboratory of Ion Beam Bioengineering, Hefei Institutes of Physical Science, Chinese Academy of Sciences
Hefei, Anhui 230031 (China)

Supporting information for this article can be found under: http://dx.doi.org/10.1002/anie.201608271.

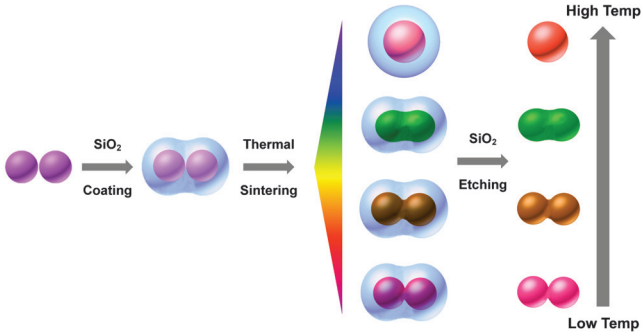

Figure 1. Schematic illustration of the shape evolution of an Ag^+ soldered AuNP dimer embedded in silica during thermal sintering. Note that a higher temperature leads to a thickened sintering neck (conductive junction).

near-infrared (NIR) I,II regions by combining in-solution Ag^+ soldering[23] and thermal sintering.[24] Our idea is to use solid-state sintering to build a conductive junction (CJ) between two AuNPs. Because the sintering temperature is far below the melting point of gold, only diffusional surface, volume, or boundary atoms can migrate (driven by reduced surface free energy) to fill the approximately 1 nm Ag^+-soldered gap.[24] This allows a facile control on the CJ width (diameter of a circular contact area) by simply altering the sintering temperature. Note that any inter-dimer sintering should be suppressed to avoid agglomeration. This is achievable by a silica-shell-isolated thermal treatment,[25] in which the silica coating serves as a nanoreactor. Last and most importantly, the inter-particle gap should be small enough so that the CJ can be easily formed. This is why a powder sample needs to be pressurized to improve sintering efficiency.[26] AuNP dimers obtained by Ag^+ soldering[23,27] nicely meet this requirement.

Our strategy contains four major steps. 1) Self-assembled dimers of AuNPs (Figure S1) are obtained by Ag^+ soldering and purified by gel electrophoresis (Figure S2).[27a] 2) The dimers are coated with protective silica shells to form dimer@SiO_2 structures; 3) The dimer@SiO_2 solutions are freeze-dried and subjected to a 15 min heating above 150 °C to form the desired CJ; 4) The silica layers are removed if necessary by dispersing the structures in a NaOH solution containing a BSPP (bis-*p*-sulfonatophenylphenyl phosphine dihydrate dipotassium) capping agent. In step 1, Ag^+ is added to a solution of AuNPs capped by BSPP to induce a self-limiting colloidal aggregation (due to BSPP striping by Ag^+)[27a] into discrete AuNP clusters in the presence of fish-sperm DNA stabilizer. Dimers are isolated by agarose gel electrophoresis (see Supporting Information).

As shown in Figure S3 in the Supporting Information, the dimer structures with or without silica coating exhibited well-resolved transverse and longitudinal LSPRs due to gap-mode plasmonic coupling.[27a] Based on the spectral data, inter-particle gaps of 0.76–1.20 nm (Figures S4 and S5) could be estimated by fitting with simulated data.[28] Redshifts of the LSPR peaks after silica coating were caused by the larger refractive index of SiO_2 (1.46) in comparison with H_2O (1.33).[1,2] Aqueous solutions of the dimer@SiO_2 structures (Figure S6) were freeze-dried to obtain fluffy powders which were then subjected to sintering at given temperatures for 15 min. TEM images in Figure 2 depict four typical morphologies of the products sintered at selected temperatures. Note that the uniform and thick silica shells revealed by TEM are important to suppress inter-dimer sintering.[25] At a relatively low temperature, a small CJ width was seen between two AuNPs. With an increased temperature, the junction became thickened. Further elevating the temperature led to a flattened sintering neck, and the dimers had a rod-like shape. At the highest temperature, a complete fusion of two AuNPs happened. The CJ widths were measured based on the TEM data of silica-removed products (Figure 3) and shown in Figure S7. It should be emphasized that no sintering happened between different dimers. The silica shells were removed to release the Au structures (Figure 3) in a hot NaOH solution mixed with BSPP, where NaOH served as an etchant for SiO_2 and BSPP was a stabilizer for gold. The silica-removed products were uniformly distributed, mirroring a good colloidal stability and product purity. The highly uniform products allowed us to measure

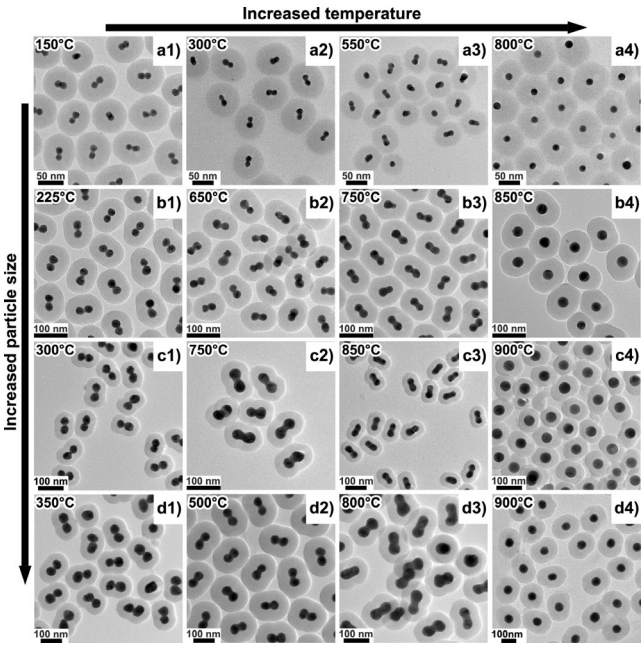

Figure 2. TEM images of silica-coated AuNP dimers sintered at different temperatures. Rows (a) to (d) correspond to increased diameters (13, 25, 35, and 45 nm) of AuNPs. Columns 1–4 correspond to increased temperatures.

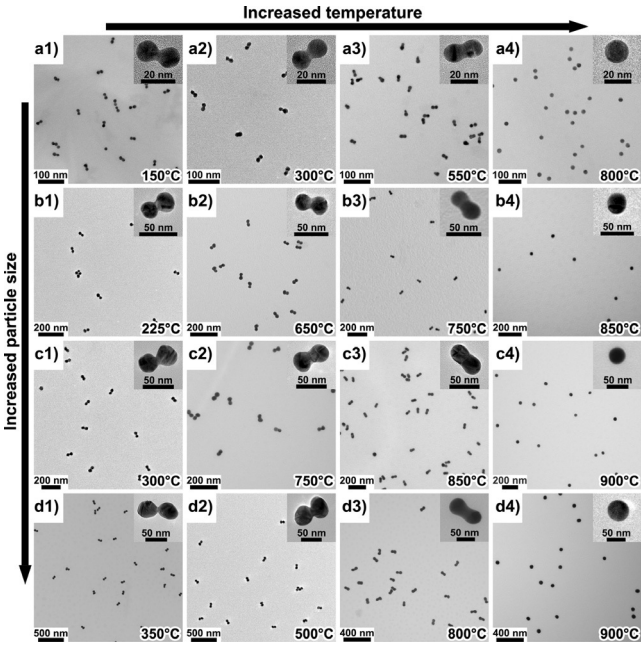

Figure 3. TEM images of silica-removed AuNP dimers sintered at different temperatures. Rows (a) to (d) correspond to increased diameters (13, 25, 35, and 45 nm) of AuNPs. Columns 1–4 correspond to increased temperatures. Insets are enlarged images of sintered dimers. See Figures S23–S38 for large-area TEM images. Note: no purifications were performed before TEM imaging.

their optical extinctions without being interfered by irrelevant aggregates.

The temperature-dictated CJ widths of the above structures resulted in very rich colors of the products (Figures S8–S11) due to the well-tuned CTP resonance, sharply different from the original capacitive plasmon (Figure S3). Optical extinctions of the dimer@SiO_2 derivatives in solution were given in Figure 4a1–a4, revealing an extremely wide tuning of the CTP up to the NIR II region. In the case of the smallest 13 nm AuNP dimer, a CTP peak at 900 nm accompanied by a weakened capacitive peak at around 600 nm was observed for a sintering at 150 °C. All the CTP peaks were blueshifted with elevated sintering temperatures as a result of widened interparticle junctions. At the highest temperature, the separated CTP peaks no longer existed due to a complete overlapping between transverse and longitudinal LSPRs. In this extreme case, two AuNPs fused into a single larger isotropic sphere, causing a degeneration of the transverse and longitudinal LSPRs due to a loss of structural anisotropy. It is noteworthy that NIR I and II domains (650–950 and 1000–1450 nm) are ideal for bio-imaging and photothermal therapy because of minimized light scattering and autofluorescence in a biological tissue.[29] Such a full spectrum tuning from 520 nm to >1300 nm is also attractive to light harvesting and photocatalysis where a good match between incidence and resonance wavelengths is critical. After silica removal, the extinction peaks shifted to shorter wavelengths (Figure 4b1–b4). One reason was the smaller refractive index of water in comparison with SiO_2. More significant shifts happened for weakly

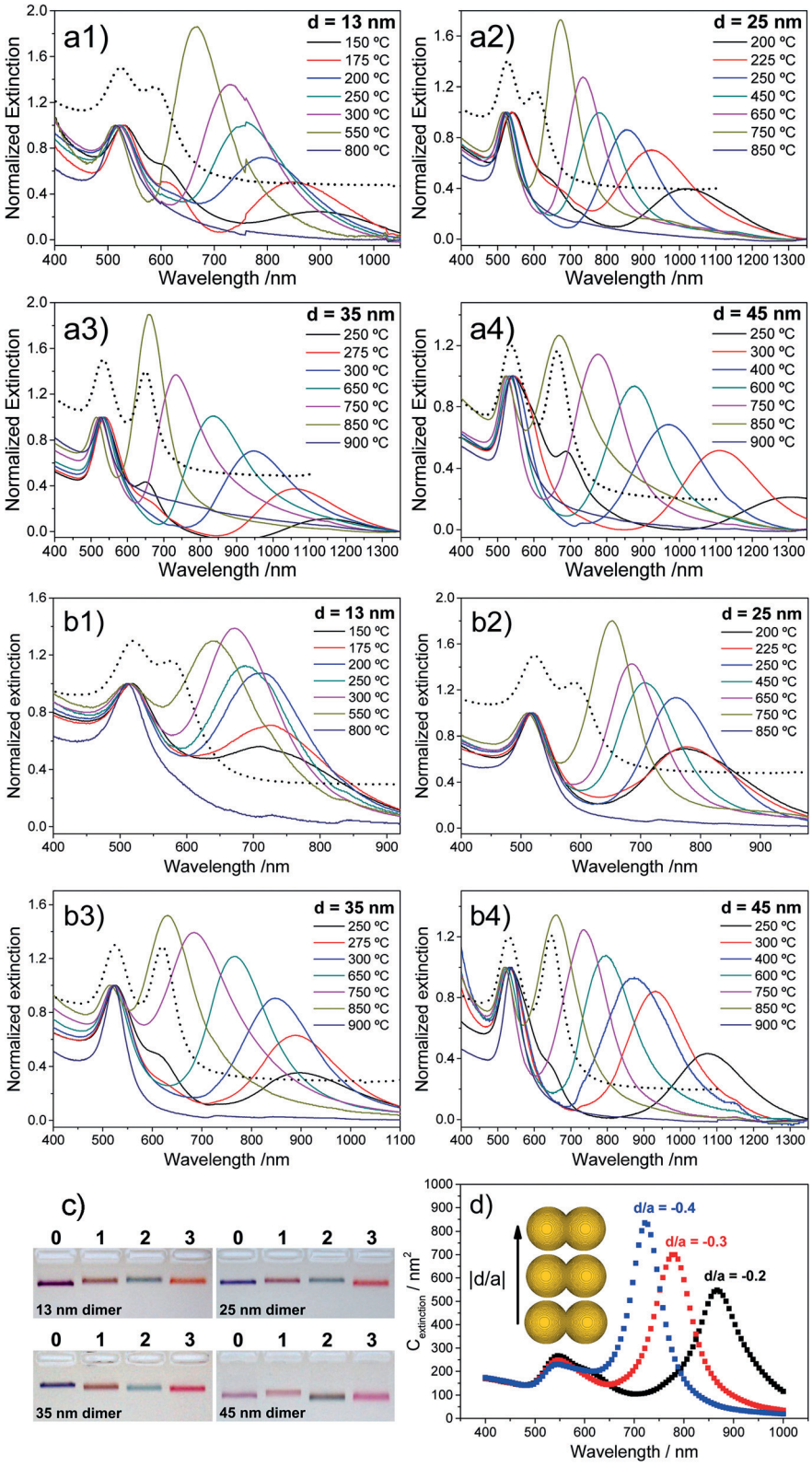

Figure 4. a,b) Normalized extinction spectra of sintered AuNP dimers of different diameters: a) before and b) after silica-shell removal. Dashed curves (vertically shifted for clarity) are spectra of unsintered AuNP dimers: a) with and b) without silica coating. c) Agarose gel electrophoreses of gel-purified and silica-removed AuNP dimers (see Figure S13 for gel patterns of original samples) sintered at different temperatures; Lanes 0 are unsintered dimers, and lanes 1–3 correspond to increased sintering temperatures: 300, 550, and 800 °C for 13 nm dimers; 650, 750, and 850 °C for 25 nm dimers; 750, 850, and 900 °C for 35 nm dimers; and 500, 800, and 900 °C for 45 nm dimers; d) Longitudinal extinction cross sections of sintered 13 nm Au dimers embedded in silica with different *d*/*a* ratios calculated by the DDA method with the electric field of polarized incident light oriented along the center-to-center line of the dimer.

sintered structures, possibly due to a "collapse" of the very narrow conductive necks which require a structural support by the silica layer. This would be especially true for smaller AuNPs where the contact area between two particles was the smallest. Upon silica removal (Figure S12), the sintered dimers showed a CTP wavelength as long as 1100 nm for the 45 nm dimers. In the case of the 13 nm dimers, the longest resonance wavelength moved to about 720 nm.

We employed agarose gel electrophoresis to further verify the size/charge uniformity and colloidal stability of the shell-removed products. Gel electrophoresis is good at inspecting colloidal structures based on their mobility and visual color without altering their native structures.[30] Structural changes do happen during TEM imaging due to dehydration and e-beam induced sample damage.[22,27a,31] Moreover, TEM cannot give a "whole picture" of a sample, which is sometimes misleading. The gel data in Figure S13 show concentrated major bands corresponding to silica-removed products. This indicated a good purity and stability of the sintered dimers. In rare cases, a weak gel band following a major product was observed, implying the existence of negligible aggregates (Figure S13). The gel-isolated products could run again in a new agarose gel as very sharp and clean bands (Figure 4c), signaling an excellent colloidal stability. Importantly, spectral profiles (Figure S14) of the gel-purified products were almost identical to the raw samples, which, along with the TEM evidences, verified that the appealing spectral features in Figure 4a,b were real reflections of the sintered dimers (not of random aggregates).

To rationalize the very large plasmonic shifts and spectral evolutions observed above, theoretical calculations were performed using a discrete dipole approximation (DDA) method.[32] The 13 nm AuNP dimer was taken as an example. To model a sintered structure, we employed two AuNPs with a center-to-center distance (L) smaller than their diameter ($2a$). This corresponded to a negative surface distance ($d = L-2a$) of a dimer. Therefore, a smaller (more negative) d/a ratio meant a larger junction width corresponding to a higher sintering temperature. The simulated longitudinal LSPR spectra ($d/a = -0.2, -0.3, -0.4$) of the coalesced 13 nm dimers surrounded by silica showed a spectral evolution (Figure 4d) consistent with our experiments as well as previous calculations with a boundary element method (BEM).[13]

Another important concern for the sintered dimers is the possibility of surface functionalization, the key to applications as self-assembly building blocks and sensing/therapeutic probes. We examined DNA oligonucleotide as a biomolecular ligand to functionalize the sintered 13 nm dimers. As shown in Figure S15, after an interaction with the thiolated DNA via Au–S bonding, the sintered dimers displayed significantly lowered gel mobility, indicating a successful DNA decoration.[30] 5 nm AuNPs mono-functionalized[30,33] with a complementary DNA sequence then hybridized with the DNA-multifunctionalized sintered structures to form core-satellite assemblies. The use of monovalent DNA-AuNP conjugate as a satellite particle would guarantee the formation of non-crosslinked assemblies.[30,34] Gel electrophoresis showed a further retarded band after hybridization with the 5 nm AuNPs (Figure S15a). The core-satellites were eluted from the gel band and subjected to TEM verifications. Figures S16a and S17 showed monodisperse core-satellites with each core surrounded by many (35 in average) satellites, benefiting from the high DNA decoration efficiency. Interestingly, when the 5 nm satellites were replaced by 13 nm ones (Figures S15b, S16b, and S18), the core particles were still distinguishable owing to their unique shape. Spectral data (Figure S19) showed a CTP at 640 nm originating from the sintered cores. These results evidenced that our process did not cause a surface passivation of the products.

We previously demonstrated an Ag^+ soldering of DNA-assembled AuNP clusters to realize DNA-programmable strong capacitive plasmonic coupling.[23] According to this success, it is natural to think about using a DNA-assembled dimer for the sintering. Continuing with this idea, it will be possible to combine our strategy with DNA-programmable nanoparticle assemblies[6] toward increased structural complexity and versatile LSPR tuning. As a preliminary test, we prepared DNA-assembled 13 nm AuNP dimers which were soldered by Ag^+ to form ≈ 1 nm interparticle gaps. Spectroscopic (Figure S20a) and TEM data (Figures S21 and S22) unambiguously verified the DNA-linked dimers and their strong coupling achieved by Ag^+ soldering.[23] The approximately 1 nm gap achieved by Ag^+ soldering was critical for the formation of a CT junction (Figures S39a and S40) between DNA-linked 13 nm AuNPs during a thermal treatment, leading to a well-defined CTP peak (Figure S20a), in sharp contrast to the unsoldered DNA-linked dimers (Figures S39b and S41).

In summary, we have developed a strategy involving Ag^+ soldering and silica-shell confined thermal sintering to achieve a precise coalescence control of nanoparticle dimers. The resulting structures exhibit a widely tunable CTP spanning an 800 nm wavelength range. Our success benefits from a perfect match between a newly developed Ag^+ soldering technique and silica-isolated thermal sintering. The resulting longitudinal LSPR is highly dependent on the sintering temperature which controls the width of the conductive sintering neck without changing the volume of the structure. The final products have a good stability in solution such that surface-functionalization by DNA is achieved for programmable nanoparticle assembly, providing novel anisotropic building blocks for DNA nanotechnology.[6] Based on our findings, some possible applications can be envisioned. For example, previous work has achieved the best Raman enhancement for coalesced AuNP dimers.[18,31b] In particular, the continuously tunable LSPR is ideal for surface-enhanced resonance Raman scattering (SERRS) for which a strict wavelength match among incidence laser, plasmon resonance, and dye absorbance is required.[35] The sintered structures with a CTP tuned to NIR are desired for nano-biomedical applications to increase light penetration depth in biological tissues.[9a,c,29a,b] The small size of our material will be advantageous owing to improved colloidal stability, facilitated in vivo clearance (reduced toxicity), and improved tumor penetration.[36] Our work is also helpful to solve the charge-transport dilemma of solution-processed materials toward bottom-up device fabrications.[17]

Acknowledgements

This work was supported by NNSFC (21425521, 21273214, and 21521001), the MOST of China (2016YFA0201300), Hefei Center for Physical Science and Technology (2014FXCX010), and the Collaborative Innovation Center of Suzhou Nano Science and Technology. We thank F.K. for her kind help with Figure 1.

Keywords: DNA self-assembly · nanodimers · nanoparticles · plasmonics · sintering

How to cite: *Angew. Chem. Int. Ed.* **2016**, *55*, 14296–14300
Angew. Chem. **2016**, *128*, 14508–14512

[1] a) E. Hutter, J. H. Fendler, *Adv. Mater.* **2004**, *16*, 1685; b) V. Giannini, A. I. Fernández-Domínguez, S. C. Heck, S. A. Maier, *Chem. Rev.* **2011**, *111*, 3888.

[2] a) S. K. Ghosh, S. Nath, S. Kundu, K. Esumi, T. Pal, *J. Phys. Chem. B* **2004**, *108*, 13963; b) A. C. Templeton, J. J. Pietron, R. W. Murray, P. Mulvaney, *J. Phys. Chem. B* **2000**, *104*, 564.

[3] a) W. Rechberger, A. Hohenau, A. Leitner, J. R. Krenn, B. Lamprecht, F. R. Aussenegg, *Opt. Commun.* **2003**, *220*, 137; b) N. J. Halas, S. Lal, W.-S. Chang, S. Link, P. Nordlander, *Chem. Rev.* **2011**, *111*, 3913.

[4] a) F. Wen, Y. Zhang, S. Gottheim, N. S. King, Y. Zhang, P. Nordlander, N. J. Halas, *ACS Nano* **2015**, *9*, 6428; b) O. Pérez-González, N. Zabala, A. G. Borisov, N. J. Halas, P. Nordlander, J. Aizpurua, *Nano Lett.* **2010**, *10*, 3090.

[5] P. Nordlander, C. Oubre, E. Prodan, K. Li, M. I. Stockman, *Nano Lett.* **2004**, *4*, 899.

[6] a) M. R. Jones, N. C. Seeman, C. A. Mirkin, *Science* **2015**, *347*, 1260901; b) A. V. Pinheiro, D. Han, W. M. Shih, H. Yan, *Nat. Nanotechnol.* **2011**, *6*, 763; c) A. Kuzyk, R. Schreiber, Z. Fan, G. Pardatscher, E.-M. Roller, A. Högele, F. C. Simmel, A. O. Govorov, T. Liedl, *Nature* **2012**, *483*, 311; d) G. P. Acuna, F. M. Möller, P. Holzmeister, S. Beater, B. Lalkens, P. Tinnefeld, *Science* **2012**, *338*, 506; e) V. V. Thacker, L. O. Herrmann, D. O. Sigle, T. Zhang, T. Liedl, J. J. Baumberg, U. F. Keyser, *Nat. Commun.* **2014**, *5*, 3448.

[7] L. A. Lane, X. Qian, S. Nie, *Chem. Rev.* **2015**, *115*, 10489.

[8] a) D.-K. Lim, K.-S. Jeon, H. M. Kim, J.-M. Nam, Y. D. Suh, *Nat. Mater.* **2010**, *9*, 60; b) X. Wu, L. Zhang, D. Lü, Y. Liu, Y. Chen, W. Su, N. Luo, R. Xiang, *Acta Chim. Sin.* **2013**, *71*, 299; c) K. Saha, S. S. Agasti, C. Kim, X. Li, V. M. Rotello, *Chem. Rev.* **2012**, *112*, 2739.

[9] a) L. Cheng, C. Wang, L. Feng, K. Yang, Z. Liu, *Chem. Rev.* **2014**, *114*, 10869; b) Y. Wang, B. Yan, L. Chen, *Chem. Rev.* **2013**, *113*, 1391; c) M. Hu, J. Chen, Z.-Y. Li, L. Au, G. V. Hartland, X. Li, M. Marquez, Y. Xia, *Chem. Soc. Rev.* **2006**, *35*, 1084; d) E. Boisselier, D. Astruc, *Chem. Soc. Rev.* **2009**, *38*, 1759.

[10] a) M. Lee, J. U. Kim, J. S. Lee, B. I. Lee, J. Shin, C. B. Park, *Adv. Mater.* **2014**, *26*, 4463; b) A. Aubry, D. Y. Lei, A. I. Fernández-Domínguez, Y. Sonnefraud, S. A. Maier, J. B. Pendry, *Nano Lett.* **2010**, *10*, 2574; c) H. J. Park, L. J. Guo, *Chin. Chem. Lett.* **2015**, *26*, 419.

[11] a) S. Linic, U. Aslam, C. Boerigter, M. Morabito, *Nat. Mater.* **2015**, *14*, 567; b) L. Zhao, Y. Huang, D. Wu, B. Ren, *Acta Chim. Sin.* **2014**, *72*, 1125; c) Y.-F. Huang, M. Zhang, L.-B. Zhao, J.-M. Feng, D.-Y. Wu, B. Ren, Z.-Q. Tian, *Angew. Chem. Int. Ed.* **2014**, *53*, 2353; *Angew. Chem.* **2014**, *126*, 2385.

[12] W. L. Barnes, A. Dereux, T. W. Ebbesen, *Nature* **2003**, *424*, 824.

[13] I. Romero, J. Aizpurua, G. W. Bryant, F. J. García de Abajo, *Opt. Express* **2006**, *14*, 9988.

[14] J. Gu, R. Singh, X. Liu, X. Zhang, Y. Ma, S. Zhang, S. A. Maier, Z. Tian, A. K. Azad, H.-T. Chen, A. J. Taylor, J. Han, W. Zhang, *Nat. Commun.* **2012**, *3*, 1151.

[15] a) N. Large, M. Abb, J. Aizpurua, O. L. Muskens, *Nano Lett.* **2010**, *10*, 1741; b) M. Abb, P. Albella, J. Aizpurua, O. L. Muskens, *Nano Lett.* **2011**, *11*, 2457.

[16] a) D. S. Sebba, J. J. Mock, D. R. Smith, T. H. LaBean, A. A. Lazarides, *Nano Lett.* **2008**, *8*, 1803; b) Y. Chen, C. Mao, *Small* **2008**, *4*, 2191; c) X. Lan, Z. Chen, B.-J. Liu, B. Ren, J. Henzie, Q. Wang, *Small* **2013**, *9*, 2308; d) L. Lermusiaux, A. Sereda, B. Portier, E. Larquet, S. Bidault, *ACS Nano* **2012**, *6*, 10992.

[17] J.-Y. Kim, N. A. Kotov, *Chem. Mater.* **2014**, *26*, 134.

[18] J.-H. Lee, M.-H. You, G.-H. Kim, J.-M. Nam, *Nano Lett.* **2014**, *14*, 6217.

[19] T. Song, L. Tang, L. H. Tan, X. Wang, N. S. R. Satyavolu, H. Xing, Z. Wang, J. Li, H. Liang, Y. Lu, *Angew. Chem. Int. Ed.* **2015**, *54*, 8114; *Angew. Chem.* **2015**, *127*, 8232.

[20] a) Y. Hu, Y. Sun, *J. Am. Chem. Soc.* **2013**, *135*, 2213; b) Y. Sun, *Natl. Sci. Rev.* **2015**, *2*, 329.

[21] T. Atay, J.-H. Song, A. V. Nurmikko, *Nano Lett.* **2004**, *4*, 1627.

[22] J. A. Scholl, A. Garcia-Etxarri, A. L. Koh, J. A. Dionne, *Nano Lett.* **2013**, *13*, 564.

[23] H. Wang, Y. Li, M. Liu, M. Gong, Z. Deng, *Small* **2015**, *11*, 2247.

[24] a) Y. U. Wang, *Acta Mater.* **2006**, *54*, 953; b) H. Djohari, J. I. Martínez-Herrera, J. J. Derby, *Chem. Eng. Sci.* **2009**, *64*, 3799.

[25] C. Gao, Y. Hu, M. Wang, M. Chi, Y. Yin, *J. Am. Chem. Soc.* **2014**, *136*, 7474.

[26] a) A. D. Albert, M. F. Becker, J. W. Keto, D. Kovar, *Acta Mater.* **2008**, *56*, 1820; b) M. N. Rahaman, *Ceramic Processing and Sintering*, Marcel Dekker, New York, **2003**.

[27] a) M. Liu, L. Fang, Y. Li, M. Gong, A. Xu, Z. Deng, *Chem. Sci.* **2016**, *7*, 5435; b) M. Liu, Q. Tian, Y. Li, B. You, A. Xu, Z. Deng, *Langmuir* **2015**, *31*, 4589.

[28] a) F. J. García de Abajo, *Phys. Rev. Lett.* **1999**, *82*, 2776; b) F. J. García de Abajo, *Phys. Rev. B* **1999**, *60*, 6086.

[29] a) R. Wang, F. Zhang, *J. Mater. Chem. B* **2014**, *2*, 2422; b) Y. Zhang, G. Hong, Y. Zhang, G. Chen, F. Li, H. Dai, Q. Wang, *ACS Nano* **2012**, *6*, 3695; c) A. M. Smith, M. C. Mancini, S. Nie, *Nat. Nanotechnol.* **2009**, *4*, 710.

[30] H. Wang, Z. Deng, *Chin. Chem. Lett.* **2015**, *26*, 1435.

[31] a) M. José-Yacamán, C. Gutierrez-Wing, M. Miki, D.-Q. Yang, K. N. Piyakis, E. Sacher, *J. Phys. Chem. B* **2005**, *109*, 9703; b) K. L. Wustholz, A.-I. Henry, J. M. McMahon, R. G. Freeman, N. Valley, M. E. Piotti, M. J. Natan, G. C. Schatz, R. P. Van Duyne, *J. Am. Chem. Soc.* **2010**, *132*, 10903.

[32] a) B. T. Draine, P. J. Flatau, *JOSA A* **1994**, *11*, 1491; b) P. J. Flatau, B. T. Draine, *Opt. Express* **2012**, *20*, 1247.

[33] D. Zanchet, C. M. Micheel, W. J. Parak, D. Gerion, A. P. Alivisatos, *Nano Lett.* **2001**, *1*, 32.

[34] a) Y. Li, Y. Zheng, M. Gong, Z. Deng, *Chem. Commun.* **2012**, *48*, 3727; b) Y. Yang, X. Bai, L. Fang, Z. Deng, *Chin. J. Chem. Phys.* **2013**, *26*, 601.

[35] A. A. Stacy, R. P. Van Duyne, *Chem. Phys. Lett.* **1983**, *102*, 365.

[36] E. Blanco, H. Shen, M. Ferrari, *Nat. Biotechnol.* **2015**, *33*, 941.

Received: August 24, 2016
Published online: October 12, 2016

